Atmósfera 20(3), 247-269 (2007)

Sensitivity of cloud albedo to aerosol concentration and spectral dispersion of cloud droplet size distribution

G. IORGA
Department of Physics and Applied Mathematics, Faculty of Chemistry, University of Bucharest, Regina Elisabeta, No. 4-12, 030018 Bucharest, Romania
Corresponding author e-mail: giorga@gw-chimie.math.unibuc.ro

S. STEFAN
Department of Atmospheric Physics, Faculty of Physics, University of Bucharest, P. O. Box MG-11, 077125 Bucharest, Romania

Received January 10, 2006; accepted October 26, 2006

RESUMEN

La reflectividad nubosa a nivel regional puede modificarse tanto por el aumento en el número de concentración del aerosol, como por el incremento en la dispersión de la distribución relativa del tamaño de las gotas de las nubes. Este trabajo se enfoca en el papel que tienen los aerosoles prenubosos en la reflectividad de las nubes. Para describir dos tipos de aerosoles, los marinos y los rurales, se utilizaron tamaños de distribución logarítmica normales. El número de aerosoles que se activan como gotas se obtuvo con base en la parametrización de activación de Abdul-Razzak y Ghan (2000). Se calculó el albedo nuboso considerando el efecto de dispersión espectral en la parametrización del radio efectivo de nubes y en el factor de asimetría de dispersión. Para considerar la dispersión se utilizaron dos factores de escalamiento diferentes. También se investigó la sensibilidad del albedo nuboso a la relación entre la dispersión espectral y el número de concentración del aerosol, en función del contenido de agua líquida (LWC) y del radio efectivo de gotas. Al considerar la dispersión se obtuvieron valores altos de radio efectivo con respecto al caso base, en el que no se considera la dispersión. Las diferencias absolutas inferidas en los valores del radio efectivo son menores a 0.8 μm al calcularlas con cada uno de los dos factores de escalamiento ya que el LWC está entre 0.1 y 1.0 g m^{-3}. Cuando la dispersión es considerada tanto en el radio efectivo como en el factor de escalamiento (factor de escalamiento βLDR) la profundidad óptica disminuye hasta 14% en el caso de los aerosoles marinos y hasta 29% en el de los continentales. En correspondencia, el cambio relativo en el albedo nuboso es de hasta 6% en el caso de las nubes marinas y hasta 11% en las continentales. Para las nubes continentales, el radio efectivo calculado considerando la dispersión se ajusta bien al rango de las mediciones de radio efectivo realizadas en el proyecto SCAR-B. El albedo nuboso calculado considerando la dispersión muestra una mejor concordancia con el albedo estimado a partir de las mediciones de radio efectivo del proyecto SCAR-B que el albedo calculado sin dispersión. En condiciones marinas despejadas de nubes, solamente el albedo escalado βLD se ajusta de manera satisfactoria al rango de validez del albedo calculado utilizando la relación radio efectivo contenido de agua líquida propuesta por Reid *et al.* (1999) en el proyecto ASTEX. El bajo coeficiente de correlación de la parametrización del radio efectivo contenido de agua líquida, también puede tener un papel.

ABSTRACT

Both the enhancement of the aerosol number concentration and the relative dispersion of the cloud droplet size distribution (spectral dispersion) on a regional scale can modify the cloud reflectivity. This work is focused on the role that pre-cloud aerosol plays in cloud reflectivity. Log-normal aerosol size distributions were used to describe two aerosol types: marine and rural. The number of aerosols that activate to droplets was obtained based on Abdul-Razzak and Ghan's (2000) activation parameterization. The cloud albedo taking into account the spectral dispersion effect in the parameterization of cloud effective radius and in the scattering asymmetry factor has been estimated. Two different scaling factors to account for dispersion were used. The sensitivity of cloud albedo to spectral dispersion-cloud droplet number concentration relationship in connection to the changes in liquid water content (LWC), and the cloud droplet effective radius has been also investigated. We obtained higher values of effective radius when dispersion is taken into account, with respect to the base case (without considering dispersion). The inferred absolute differences in effective radius values between calculations with each of the scaling factors are below 0.8 μm as LWC ranges between 0.1 and 1.0 g m^{-3}. The optical depth decreased by up to 14% (marine), and up to 29% (continental) when dispersion is considered in both effective radius and asymmetry factor (β_{LDR} scaling factor). Correspondingly, the relative change in cloud albedo is up to 6% (marine) and up to 11% (continental) clouds. For continental clouds, the calculated effective radius when dispersion is considered fits well within the measured range of effective radius in SCAR-B project. The calculated cloud albedo when dispersion is considered shows better agreement with the estimated cloud albedo from measured effective radius in SCAR-B project than the cloud albedo calculated without dispersion. In cleaner conditions of marine clouds, only β_{PL}-scaled albedo fits satisfactory within the validity range of albedo inferred using an effective radius-liquid water content relationship proposed by Reid *et al.* (1999) from ASTEX project. The low correlation coefficient of the effective radius-liquid water content parameterization in ASTEX may also play a role within.

Keywords: Aerosol size distribution, spectral dispersion, effective radius, cloud albedo, indirect aerosol effect.

1. Introduction

Aerosols are multi-component particles, consisting mainly of sulfate, nitrate, ammonium, black carbon, primary and secondary organic mater, in submicron size range, and sea salt, mineral dust, primary organic mater, nitrate, in supermicron size range (Putaud *et al.*, 2004). Concentrations of trace elements such as sodium, cesium, chloride, copper, silver, cadmium, lead, nickel, zinc, iron, mercury, and manganese have been also identified in fine particles. Common elements in the coarse range include silicon, aluminum, iron, potassium, calcium, magnesium, and other alkaline and transition elements (Godish, 1997). Particles properties (e.g. mass/number concentration, size distribution, absorptive characteristics) determine how atmospheric aerosols alter the Earth's radiation balance thereby having an impact on climate.

Aerosols have a direct radiative forcing (e.g. Charlson *et al.*, 1992; Haywood and Shine, 1995) by scattering and absorbing solar radiation and by absorbing and emitting thermal radiation. This can lead to either a cooling (e.g. sulfates, nitrates...) or a warming (black carbon) of the atmosphere depending on the proportion of scattered light to that absorbed. In addition to the direct forcing, aerosols perturb the radiation balance indirectly, through the formation of clouds because aerosols can serve as cloud condensation and/or ice nuclei. In polluted regions, an increased aerosol concentration can modify the microphysical and radiative properties of clouds (first aerosol in-

direct effect; Twomey, 1974), as well as the precipitation efficiency and hence the cloud lifetime (second aerosol indirect effect; Albrecht, 1989; Pincus and Baker, 1994). Both, first and second indirect effects of aerosols on climate are believed to increase the amount of solar radiation that is reflected into space without reaching the Earth's surface, resulting in a cooling effect. The third climatic effect of aerosols is linked to the presence of absorbing components in aerosol particles; these particles absorb radiation and the resulting radiative heating in elevated layers can perturb the temperature profile, which can lead to the evaporation of low-level clouds (semi-direct effect; Hansen *et al.*, 1997; Ackerman *et al.*, 2000). The Intergovernmental Panel on Climate Change report (2001) estimated the direct forcing of anthropogenic aerosols to be −0.5 W m^{-2} and the total indirect forcing to lie between 0 and −2 W m^{-2}, in global mean. The resulting total radiative forcing (well-mixed greenhouse gases, solar activity, ozone, direct aerosol effects and Twomey effect) has a 75-97% probability of being positive (McFiggans *et al.*, 2006). This latest estimate neglects the cloud lifetime effect and aerosol effects on mixed-phase and ice clouds because the scientific knowledge about these latter effects is not sufficient to predict their magnitudes yet.

Recent reviews of theoretical and observational evidence for the aerosol effects can be found for instance in the work of Haywood and Boucher (2000), in IPCC (2001), in the works of Kanakidou *et al.* (2005), Lohmann and Feichter (2005), and Yu *et al.* (2006); while McFiggans *et al.* (2006) review the currently-available observational evidence for the compositional complexity of atmospheric aerosol, and the derived properties of their size distributions and composition that are thought to affect aerosol ability to act as cloud condensation nuclei (CCN). All these studies point out that amongst aerosol effects, the indirect one is currently credited with the greatest range of uncertainty.

Existing GCM-based calculations tend to overestimate the indirect aerosol effect as they use many simplifications imposed by the large number of coupled processes, over a large range of spatial and temporal scales that need to be addressed, in order to deal with the associated computational burden. Lohmann and Feichter (2005) estimate for the cloud albedo effect values between −1.9 and −0.5 Wm^{-2}, and between −1.4 and −0.3 Wm^{-2} for the cloud lifetime effect. The poor aerosol characterization in GCM is in part due to the lack of a comprehensive global database of aerosol concentrations, chemical composition and optical properties; subtle aspects of the interaction between aerosols and clouds are not entirely captured (Haywood and Boucher, 2000). Therefore, the uncertainty in the estimations is mostly attributed to the complex issues regarding the link aerosol particles-cloud droplets, like the aerosol and aerosol precursor emissions from a given emission inventory, like the representation of aerosol size distribution (Ghan *et al.*, 2001a), and the cloud nucleation parameterization (e.g., Boucher and Lohmann, 1995), the relationship between effective radius and volume mean radius (Chen and Penner, 2005) and the representation of the microphysics of mid-level clouds (Lohmann *et al.*, 2000). The great computational expense associated with detailed simulations of relevant phenomena also prevents reliable assessments of the forcing with regional and global atmospheric models.

Currently, there are two categories of approaches to relate the aerosol properties (concentration, size and composition) to the cloud microphysical properties (number concentration and effective radius): the empirical approach and the mechanistic one.

First approach uses an empirical relationship between cloud droplet number and aerosol mass concentration (Boucher and Lohmann, 1995; Roelofs *et al.*, 1998; Menon *et al.*, 2002; Lowenthal, 2004). At present, such relationships can only be derived between sulfate aerosols, sea salt, organic carbon and cloud droplet number, but data are not available yet for dust or black carbon and cloud droplet number. These methods are based on observations and are easy to use in global forcing calculations, but they do not reflect the physical and chemical processes that occur during cloud nucleation, which depend on the size, chemical composition of the aerosol, as well as the updraft velocity. In addition, they are based on measurements at particular regions and times, therefore it is questionable if they could be used for a global calculation or used to simulate future climates.

As the primary source of cloud droplets is droplet nucleation, which depends on the aerosol size distribution, composition and the updraft velocity, the mechanistic approach considers these important aspects. Abdul-Razzak *et al.* (1998) and Abdul-Razzak and Ghan (2000) developed a parameterization based on Koehler theory that can describe the cloud droplet formation for a mono- and a multi-modal aerosol consisting of few chemical species. This approach has been extended by Nenes and Seinfeld (2003) to include kinetic effects for aerosols that do not have time to grow to their equilibrium size. As the aerosol composition is important in cloud droplet activation in warm clouds, the effect of surface-active organics has recently been included in the parameterization of cloud droplet formation by Abdul-Razzak and Ghan (2004), while other effects of organics, such as their film-forming ability are considered by Rissman *et al.* (2004), and Fountoukis and Nenes (2005). Lance *et al.* (2004) explored the relative importance of the chemical effects of film forming compounds and of updraft velocity on cloud droplet number.

Current uncertainties in model treatments of the aerosol effects also include limitations due to dispersion of the resulted cloud droplets. Recently, Liu and Daum (2002) and Rotstayn and Liu (2003) showed that the dispersion of the cloud droplet spectrum is related to the cloud droplet number concentration. They compiled measurements in polluted and unpolluted warm stratiform and shallow cumulus clouds southwest of San Diego, over the northeastern Pacific, the northeastern Atlantic, the Southern Ocean, the eastern Florida coast, west of California, and over the northern Indian Ocean. From there, they concluded that polluted clouds with a higher droplet concentration tend to have a larger relative dispersion, other factors being the same. This simultaneous increase of the relative dispersion and droplet concentration with the increased aerosol loading may be due to a more complex chemical heterogeneity of anthropogenic aerosols, a broader size distribution, more small droplets competing for water vapor in polluted clouds compared to clean clouds, or a combination of the three (Srivastava, 1991; Wood *et al.*, 2002; Hudson and Yum, 1997; Feingold and Chuang, 2002). Pre-cloud aerosol and dynamical properties of clouds, such as updraft velocity and turbulence, may also affect the cloud droplet concentration and spectral dispersion. A relationship to include them has been proposed by Liu *et al.* (2006) very recently. However, how aerosol loading affects the cloud droplet dispersion is not clear yet, as Lu and Seinfeld (2006) provide reasons for a decrease of relative dispersion of droplet spectrum with increasing aerosol concentration when this is below 1000 cm^{-3}.

Most GCM-based calculations of indirect forcing do not consider the effect of cloud droplet dispersion and there are only few simulations (Liu and Daum, 2002; Peng and Lohmann, 2003; Rotstayn and Liu, 2003; Chen and Penner, 2005) that made it. All are focused on global mean value of indirect forcing and show that the change in the indirect forcing associated to a change from the fixed coefficient β (a coefficient between volume mean radius and effective radius (Martin *et al.*, 1994)) to a β that is related to droplet number is of some importance. The reduction of the indirect effect by including the dispersion effect is 15% by Peng and Lohmann (2003), between 12 and 35% by Rotstayn and Liu (2003), and 18% by Chen and Penner (2005).

While all estimations are within the range (10-80%) suggested by Liu and Daum (2002), there are differences in the applied methodology, the used models, parameterizations and input data. We point out here only the most important differences. The Rotstayn and Liu's (2003) model uses assumed values for pre-industrial and modern-day emissions of sulfate as a surrogate for all aerosols and infers droplet number from Boucher and Lohmann´s (1995) parameterization, includes an interactive treatment of the tropospheric sulfur cycle and a physically based cloud scheme. Peng and Lohmann's (2003) model uses cloud droplet data from RACE and FIRE.ACE field campaigns, and ECHAM4 GCM. Chen and Penner (2005) assumed a single mode log-normal size distribution for the aerosol (pure ammonium sulfate) with a total aerosol number concentration of 1000 cm^{-3}, mode radius of 0.05 μm and a standard deviation of 2, and the sectional representation of the activation scheme of Abdul-Razzak and Ghan (2002). There are differences between the parameterizations of β coefficient, as well. In all simulations, the asymmetry factor has been considered having a fixed value. None included the variation of β in the asymmetry factor.

More work is needed to understand to what extent cloud reflectivity is influenced by the spectral dispersion of cloud droplet spectrum as a function of pre-cloud aerosol via the cloud nucleation process. The aim of this study was to estimate the cloud albedo as a function of specified aerosol properties and to investigate its variability with respect to the relative dispersion of the cloud droplet size distribution (spectral dispersion). The calculated number of nucleated droplets for marine and rural aerosols was used as input for a simple cloud model to estimate the cloud optical parameters. The dispersion effect has been considered through a perturbation in effective radius with scaling factor β. We explored the difference between the cloud optical parameters associated with each perturbation to provide the measure that dispersion plays on cloud reflectivity.

2. Data description and methodology

2.1 Aerosol size representation and chemical composition

Due to the spatial and temporal variability of anthropogenic aerosols (Andreae, 1995; Jonas, 1995) the forcing has strong regional character (Kiehl and Rodhe, 1995; Ramanathan, 2001; Chameides *et al.*, 2002), and the result is a regionally heterogeneous climate response (Taylor and Penner, 1994). In view of the large regional variability of aerosol, it is questionable whether the global mean forcing is sufficient to characterize the radiative impact of aerosols and the regional scale would not be more appropriate. Therefore, two aerosol types: marine and rural (as clean-continental) have been considered. The multimode log-normal aerosol number size distributions are given by:

$$\frac{dn_a}{d\log a} = \sum_{i=1}^{3} \frac{n_{a,i}}{\sqrt{2\pi}\log\sigma_i} \exp\left(-\frac{\log(a/a_{mi})^2}{2(\log\sigma_i)^2}\right) \quad (1)$$

where $n_{a,i}$, a_{mi} and σ_i are the total number concentration, geometric mean dry radius, and geometric standard deviation of aerosol mode *i,* respectively, and a represents the aerosol particle radius.

The modal representation has been used in regional and global aerosol models (e.g., Giorgi, 1986; Binkowski and Shankar, 1995; Environmental Protection Agency (EPA), 1999; Ghan *et al.*, 2001a, 2001b, 2001c).

Measurements reported in literature show that the continental aerosol contains 15-30% sulfate, while marine aerosol contains somewhat more (30-60%), percentages that assure that fine aerosols at usual humidities are hygroscopic ones and they behave as optically ideal droplets. Beside chemical species that dissolve easily into water, atmospheric aerosol particles contain numerous substances, which are partially or completely insoluble. In this respect, we assumed that rural aerosol is a mixture of ammonium sulfate (75%) and mineral dust (25%), and pure ammonium sulfate for marine aerosol. The corresponding coefficients of the aerosol number size distributions are shown in Table Ia and result from measurements (Jaenicke, 1988; Hoppel and Frick, 1990; Bott, 2000).

The curvature parameter A and the hygroscopicity B were obtained considering the properties of each chemical component presented in Table Ib (from Qian *et al.*, 2003); for the mixed composition of rural aerosol, A and B were obtained following the procedure explained in section 2.2.

Table Ia. Modal parameters of number size distributions for marine and rural aerosol, and the radius of the smallest activated particle a_{ci} for each aerosol mode *i*.

Aerosol type	Aerosol mode	$n_{a,i}$ (cm^{-3})	a_{mi} (μm)	log σ	a_{ci} (μm)
Marine aerosol	I	100	0.027	0.25	0.046
	II	120	0.105	0.11	0.095
	III	6	0.210	0.45	0.137
Rural aerosol	I	6 650	0.007	0.225	0.116
	II	147	0.027	0.557	0.173
	III	1 990	0.042	0.266	0.224

Table Ib. For each aerosol chemical component: ν = number of ions into the salt dissociates, φ = osmotic coefficient, δ = soluble mass fraction, M_a = molecular weight, ρ_a = density, A = curvature parameter, B = hygroscopicity.

Component	ν	φ	δ	M_a	ρ_a	A	B
Ammonium sulfate	3	0.7	1.0	132	1.77	0.019	0.51
Mineral dust	-	-	0.13	-	2.60	0.019	0.14

2.2. Aerosol activation model

The processes that determine aerosol activation and droplet nucleation have been well understood and the Koehler theory expresses the number of particles activated in terms of supersaturation S, and predicts the time evolution of S in a rising air parcel (Pruppacher and Klett, 1997). A number of numerical models have been developed to implement this theory (e.g. Lee *et al.*, 1980; Flossman *et al.*, 1985; Heymsfield and Sabin, 1989), but they require detailed calculations over multiple size sections and multiple time steps between initial saturation and peak supersaturation, S_{max}, and thus they are computationally too expensive to be used in multi-dimensional atmospheric models. Therefore, several parameterizations with simplifying assumptions have been developed (e.g. Twomey, 1959; Ghan *et al.*, 1993; Abdul-Razzak *et al.*, 1998).

This study uses the parameterization of Abdul-Razzak *et al*. (1998) and Abdul-Razzak and Ghan (2000). An air parcel having specified aerosol size distribution and initial temperature, pressure and relative humidity (slightly below 100%) rises adiabatically with a specified updraft velocity. The particles whose critical or activation supersaturations (S_{crit}) are below S_{max} (achieved by the rising air parcel) are then assumed to be activated (Nenes *et al.*, 2001). This S_{max} is then used to compute the number (or the mass) of activated particles. Hereby the computational problem reduces to the calculus of S_{max}.

The generalized Abdul-Razzak and Ghan (2000) parameterization is fully described in Abdul-Razzak and Ghan (2000), therefore we revisit here only the basics, keeping in mind that for multi-mode aerosol we need to add over all modes " i " of the aerosol size distribution.

For a single aerosol type, and a single log-normal mode, the fraction of aerosol particles that activate to droplets, following Abdul-Razzak and Ghan (2000) parameterization, is given by:

$$\frac{N}{N_{ap}} = \frac{1}{2}\left[1 - erf(u)\right], \tag{2}$$

where

$$u = \frac{\ln(a_c / a_m)}{\sqrt{2}\ln\sigma},$$

N is the droplet number concentration, N_{ap} is the total aerosol number concentration, a_c is the dry radius of the smallest activated aerosol, a_m is the geometric mean radius, σ is the geometric standard deviation of the size distribution and *erf*(u) is the error function. The radii a_c and a_m are calculated from Koehler theory through their corresponding critical supersaturations: the maximum supersaturation S_{max} corresponding to the smallest activated particle a_c is given by:

$$S_{\max} = \frac{2}{\sqrt{B}}\left(\frac{A}{3a_c}\right)^{3/2} \tag{3}$$

and the critical supersaturation S_m of a particle with radius a_m, which is given by:

$$S_{\mathrm{m}} = \frac{2}{\sqrt{B}}\left(\frac{A}{3a_m}\right)^{3/2} \tag{4}$$

In the equations (3) and (4), the coefficient A counts for the curvature effect on the droplet surface and the coefficient B describes, depending on the particle composition, the hygroscopic properties of the aerosol population:

$$A = \frac{2\tau M_W}{\rho_W RT} \tag{5}$$

and

$$\mathrm{B} = \frac{\nu\phi\delta M_{\mathrm{W}}\rho_{\mathrm{a}}}{M_{\mathrm{a}}\rho_{\mathrm{W}}} \tag{6}$$

where M_{w}, M_{a} are the molecular weight of water and aerosol, ρ_{w}, ρ_{a} are the densities of water and aerosol, τ is the surface tension of water, ν is the number of ions the salt dissociates into within the water, ϕ is the osmotic coefficient, δ is the mass fraction of the soluble material, T is the temperature.

For the multimode version of the activation, the Abdul-Razzak and Ghan (2000) parameterization assumes that internal mixtures of material compose each mode; this involves that only the hygroscopicity B changes in a mean hygroscopicity parameter, averaged over all components j in aerosol mode i:

$$\mathrm{B}_{\mathrm{mix}} = \frac{M_{\mathrm{W}}\sum_{\mathrm{j=1}}^{\mathrm{J}} \mathrm{r}_{\mathrm{ij}}\nu_{\mathrm{ij}}\phi_{\mathrm{ij}}\delta_{\mathrm{ij}} / M_{\mathrm{aij}}}{\rho_{\mathrm{w}}\sum_{\mathrm{j=1}}^{\mathrm{J}} \mathrm{r}_{\mathrm{ij}} / \rho_{\mathrm{aij}}} \tag{7}$$

where r_{ij} is the mass mixing ratio of component j and mode i.

The maximum parcel supersaturation is obtained in Abdul-Razzak and Ghan (2000) parameterization using two functions $\mathrm{f}_1(1\mathrm{n}\,\sigma) = 0.5\exp\{2.5\,(1\mathrm{n}\,\sigma)^2\}$, and $\mathrm{f}_2(1\mathrm{n}\,\sigma) = 1 + 0.25\,1\mathrm{n}\,\sigma$ which are used to fit the ratio of S_{m} and $\mathrm{S}_{\mathrm{max}}$ to a numerical solution of the governing equations:

$$\left(\frac{\mathrm{S}_{\mathrm{m}}}{\mathrm{S}_{\mathrm{max}}}\right)^2 = \mathrm{f}_1(\ln\sigma)\left(\frac{\xi}{\eta}\right)^{3/2} + \mathrm{f}_2(\ln\sigma)\left(\frac{\mathrm{S}_{\mathrm{m}}{}^2}{\eta + 3\xi}\right)^{3/4} \tag{8}$$

where:

$$\eta = \frac{(\alpha\mathrm{V}/\mathrm{G})^{3/2}}{2\pi\rho_{\mathrm{W}}\gamma\mathrm{N}_{\mathrm{a}}} \tag{9}$$

$$\xi = \frac{2\mathrm{A}}{3}\left(\frac{\alpha\mathrm{V}}{\mathrm{G}}\right)^{1/2} \tag{10}$$

Here V is the updraft velocity, G accounts for diffusion of heat and moisture to the particles, α and γ are coefficients in the supersaturation balance equation (Abdul-Razzak *et al.* (1998) and Abdul-Razzak and Ghan (2000) or Pruppacher and Klett (1997) for full description).

When the aerosol population is described by a multi-modal size distribution, for each mode there is an activation cut-off size (i.e., the size of the smallest particle activated) at which $S_{crit} = S_{max}$. The number (or mass) of particles activated is the number (or mass) of particles larger than this cut-off size, and is easily calculated from the log-normal distribution. S_{max} is then obtained using the modal parameterization for a single mode. The aerosol activation predicted by this approach is in very close agreement with the explicit S_{max} module (Zhang *et al.*, 2002).

2.3 Simple cloud model: effective radius, optical depth and albedo calculations

In a global or in a regional climate model, the properties of clouds are computed in terms of optical depth, single-scattering albedo, and asymmetry factor over a number of spectral intervals (e.g., Slingo, 1989). These properties depend on the effective droplet radius and the cloud liquid water path.

The cloud droplet effective radius r_{eff}, defined by Hansen and Travis (1974) as the ratio between the third to the second moment of a droplet size distribution, depends on droplet number concentration (N) and LWC (Martin *et al.*, 1994):

$$r_{eff} = \beta \left(\frac{3}{4\pi\rho_W} \cdot \frac{LWC}{N} \right)^{1/3} \tag{11}$$

where β is a scaling coefficient frequently used in GCM to obtain r_{eff} from volume mean radius. Rotstayn and Liu (2003) suggest that β to be called spectral shape factor as it describes the width of the cloud droplet size distribution (eq. 12).

Martin *et al.* (1994) have shown that the relationship between r_{eff} and volume mean radius varies from ocean to land, and they proposed for β a value of 1.077 over ocean and of 1.143 over land, as this resulted from measurements in warm stratocumulus clouds during observations in Pacific, Atlantic and around British Isles. The cloud droplet number concentrations up to 200 cm^{-3} in clouds over ocean areas and up to 450 cm^{-3} in clouds over land were encountered.

From analysis of measurements in polluted and unpolluted warm stratiform and shallow cumulus clouds over worldwide, Liu and Daum (2002) and Rotstayn and Liu (2003) have shown that β is an increasing function of the relative dispersion ε of cloud droplet spectrum:

$$\beta_{LDR} = \frac{(1+2\varepsilon^2)^{2/3}}{(1+\varepsilon^2)^{1/3}} \tag{12}$$

where the variation of ε with N is described by

$$\varepsilon = 1 - 0.7\exp(-\lambda N) \tag{13}$$

They propose $\lambda = 0.001, 0.003, 0.008$ for the lower bound, average and upper bound of this variation respectively. The cloud droplet number concentrations they compiled were up to 800 cm^{-3}.

Peng and Lohmann (2003) had cloud data from two field campaigns: The Radiation, Aerosol and Cloud Experiment (RACE), which took place from August to October 1995 off the coast of Nova Scotia, and the First ISCCP Regional Experiment-Arctic Cloud Experiment (FIRE.ACE), that was conducted in April 1998 in the Canadian and the United States, Arctic; data that encompasses cloud droplet number concentrations up to 300 cm^{-3}. They propose to use for β its direct dependence of cloud droplet number:

$$\beta_{PL} = 1.18 + 4.5 \times 10^{-4}\ N \tag{14}$$

For warm stratocumulus cloud we considered, the cloud optical depth can be approximated (e.g., Peng *et al.*, 2002) as:

$$\tau = \frac{3}{2}\frac{LWC \cdot H}{r_{eff} \cdot \rho_W} \tag{15}$$

where H is the thickness of model layer (cloud thickness) and can be related to r_{eff} and cloud droplet number concentration N as:

$$\tau = \frac{2\pi r_{eff}^2 N \cdot H}{\beta^3} \tag{16}$$

The cloud albedo (A) was computed taking into account the two-stream approximation of a non-absorbing, horizontally homogeneous cloud (Lacis and Hansen, 1974):

$$A = \frac{\sqrt{3}(1-g)\tau}{2+\sqrt{3}(1-g)\tau} \tag{17}$$

First, we considered that the scattering asymmetry factor g has a fixed value (0.85), and second, we included the dependence of g of the cloud droplet effective radius, as in some GCM or regional climate models may be implemented. We used the parameterization in ECHAM GCM (Boucher and Lohmann, 1995) for visible range of electromagnetic spectrum:

$$g(r_{eff}) = 0.79 + 0.11 \cdot \log r_{eff} - 0.03 \cdot (\log r_{eff})^2 \tag{18}$$

The exact procedure used in the present study is as follows: 1) specify the average aerosol physical and chemical characteristic for two typical environments (rural as clean continental and marine) based on published observations, 2) determine a likely droplet number concentration based on the ARG parameterization and determine the scaling coefficient β counting for dispersion of the cloud droplet spectrum, 3) calculate the cloud effective radius, optical depth and cloud albedo in two pairs of calculation: β-scaled (denoted in figures as $+\beta$) and non-scaled (denoted in figures as $-\beta$), and estimate the differences.

3. Results and discussion

3.1 Comparison of the observed cloud droplet concentrations and model results

The number size distribution for marine, and rural aerosol calculated from parameters in Table Ia are represented in Figure 1. The number concentration of droplets nucleated in a cloud has been estimated following the procedure in section 2.2. The computations based on equations (1) ÷ (10) consider a temperature of 21 °C, and an updraft velocity of 0.5 m s^{-1} (within the expected range of stratiform clouds (Paluch and Lenschow, 1992; Seinfeld and Pandis, 1998)). The other coefficients are listed in Tables, Ia and b, and the coefficients counting for gas kinetic effects being that used by Abdul-Razzak and Ghan (2000). Using a single updraft velocity for the entire grid cell is a simplification, since the updraft velocity varies over the grid cell (Lohmann *et al.*, 1999); but we assumed it constant, since we are only interested in the cloud drop activation process, which generally occurs on the order of seconds.

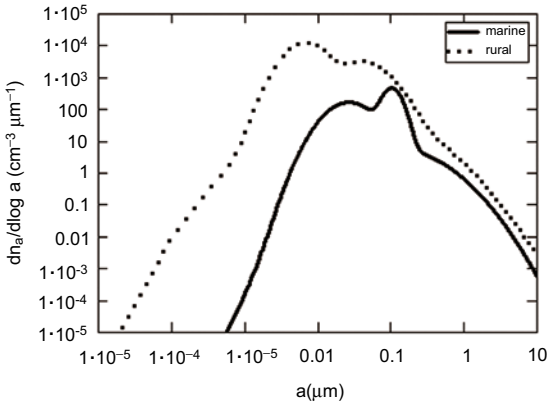

Fig. 1. Aerosol number size distributions: marine (solid line) and rural (dotted line).

Table Ia also shows the cut-off activation diameters for particles in each mode of the size distribution. Continental aerosol particles require larger particle radii for activation than the marine aerosols, indicating the presence of insoluble material in the particles. We inferred total droplet number concentrations of 60 cm^{-3} in marine case and of 319 cm^{-3} in rural case. The total aerosol number concentration is roughly 39 times larger over rural areas than over marine areas, whereas the cloud droplet number is 5 times larger in rural case. It indicates that the fraction of aerosols activated is larger for marine clouds.

As a dataset on measured droplet concentrations was not available for the size distributions considered by us, we compared our results with reports from field campaigns. Table II lists the cloud droplet number concentration values calculated using the aerosol concentration-cloud droplet concentrations relationships based on five field measurements reported by Gultepe and Isaac (1999). There were more than ten thousand observations collected over a period of 11 years in primarily stratus and stratocumulus, therefore they cover a wide range of conditions of cloud formation. We also have chosen to compare our results with that inferred from the Gultepe and Isaac (1999) correlations as these are currently being used in GCM.

Mean values from a comprehensive observational database for marine and continental stratus and stratocumulus clouds performed by Miles *et al.* (2000) are also indicated. A comparison of our cloud droplet number concentrations with that inferred from Gultepe and Isaac (1998) correlations and datasets compiled by Miles *et al.* (2000) shows a good agreement.

Table II. Cloud droplet concentration inferred from field measurements and the calculated in the present study.

Field project	Marine	Rural
Syracuse [a]	158	481
EMEFS I	107	697
EMEFS II	54	563
NARE	107	376
RACE	111	357
Miles *et al.* (2000) [b]	74	288
Present study	60	319

[a]The Syracuse project was performed in New York State during 1984. The Eulerian Model Evaluation Field Study was conducted in southern Ontario during 1988 (EMEFS I) and 1990 (EMEFS II). The North Atlantic Regional Experiment (NARE) was conducted in Nova Scotia during 1993. The Radiation, Aerosol and Cloud Experiment (RACE) took place over the Bay of Fundy and central Ontario during 1995.

[b]The database of Miles *et al.* (2000) covers *in situ* measurements and fields experiments in marine and continental stratus and stratocumulus clouds performed over 20 years.

3.2 Dispersion effect on effective radius

We investigated the influence of dispersion on droplet effective radius as LWC ranges from 0.1 to 1 g m^{-3} using the value of 0.42 for relative dispersion (ε) for marine case and that of 0.73 for rural case. The relative dispersions were inferred from the cloud droplet concentrations using first Liu and Daum (2002) and Rotstayn and Liu (2003) relationships, i.e. eqs. 12 and 13, and second using Peng and Lohmann (2003) relationship, i.e. eq. 14. This means that scaling factor β_{LDR} (respectively β_{PL}) ranges from 1.16 (1.207) for marine to 1.41 (1.324) for rural air masses; when dispersion is not considered $\beta = 1$.

The database of Miles *et al.* (2000) reveals that droplet size distributions measured in ambient conditions have relative dispersions between 0.15 and 0.83 for marine clouds, with 55% distributions having ε above 0.4, and 74% having ε above 0.3. From the same database, for clouds over land, the relative dispersions range from 0.21 to 0.9, with only 10% distributions having ε above 0.7 and 31% having ε above 0.5.

Figure 2 shows the comparison of the calculated β-scaled effective radius and non-scaled effective radius for marine and continental clouds using the above method. For an LWC ranging from 0.1 to 1 g m^{-3}, the β_{LDR}-scaled effective radius increases from 8.5 to 18.4 μm for marine clouds, and from 5.9 to 12.8 μm for continental clouds. The estimated β_{PL}-scaled effective radius is higher than β_{LDR}-scaled effective radius for marine clouds; for continental clouds, the situation is reversed. This is due to the difference in the mathematical form of the β-N relationship (for N between about

130 and 970 cm^{-3}, $\beta_{PL} > \beta_{LDR}$). In both cases, the absolute differences are below 0.8 μm as LWC ranges between the specified limits.

We estimate a measure of the dispersion effect on effective radius by defining the percentage difference δr_{eff} as:

$$\delta r_{eff} = 100 \frac{r_{eff,\beta} - r_{eff}}{r_{eff}} \tag{19}$$

where $r_{eff,\beta}$ is effective radius value when the dispersion is considered. The dispersion presence (through scaling factor β_{LDR}) leads to an increase in effective radius of 16% (marine) and respectively of 41% (continental). When scaling factor β_{PL} is used, the δr_{eff} changes to 20% (marine) and to 32% (continental). This means the effect of dispersion is more pronounced as the cloud droplet number concentration (determined by the aerosol number concentration) has higher values but the option of the β-scaling factor also plays a role.

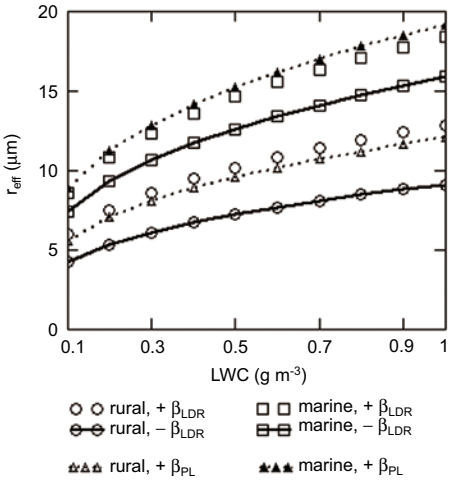

Fig. 2. Comparison of the calculated β_{LDR}-scaled (Liu and Daum relationship, eq. 12) effective radius (squares-marine, $+\beta_{LDR}$, circles-continental, $+\beta_{LDR}$) and non-scaled effective radius for marine (connected squares, $-\beta_{LDR}$) and continental clouds (connected circles, $-\beta_{LDR}$). β_{PL}-scaled effective radius (Peng and Lohmann relationship; eq 14) for both marine (dotted line, full triangles) and continental clouds (dotted line, open triangles) is also presented.

In the Earth's atmosphere a large variety of droplet sizes can be found depending very much on the type of cloud they are embedded in. Stephens (1978) quotes radii ranging from 2.25 μm for stratus clouds to 7.5 μm for stratocumulus. Han *et al.* (1994) derived radii for water clouds from satellite measurements ISCCP between 8.2 and 12 μm, but is difficult to use them for comparison with our data as information about the value of LWC is necessary. An example of a more appropriate comparison is the following: Miles *et al.* (2000) reports effective radius of 11.4 μm for marine stratocumulus when LWC = 0.28 g m^{-3}, and we calculated a β_{LDR}-scaled value of 12.3 μm at LWC = 0.3 g m^{-3}; for continental stratocumulus, Miles *et al.* (2000) provides effective radius of 9.1 μm for an LWC = 0.4 g m^{-3} for marine stratocumulus, and we calculated a β_{LDR}-scaled value of 9.43 μm. But from the same database, we extracted for LWC = 0.11 g m^{-3}, measured values of 12.7 and 4.85 μm, while we calculated β_{LDR}-scaled value of 5.94 μm and a non-scaled value of 4.21 μm. This is as indication that while the differences between the measurements can be attributed to the

different sampling locations, methods and the meteorological parameters, our simulations can not be directly compared with this database. A further comparison is performed in section 3.5.

3.3 Dispersion effect on cloud albedo

According to equations (11-17), an increase in ε acts to decrease the optical depth and the cloud reflectivity. In the following calculations the cloud albedo is calculated in the assumption that the scattering asymmetry factor has a fixed value of 0.85.

In both cloud types, there is a decrease in optical depth (Fig. 3) and cloud albedo (Fig. 4), as liquid water increases and as spectral dispersion increases. This behaviour varies with aerosol type, the decrease (defined in the same way like δr_{eff}) in optical depth being of up to 14 (17%) in the marine case, and up to 29 (24%) in the rural case for a cloud of 100 m thickness (β_{LDR}, respectively β_{PL} were used). When spectral dispersion is represented by β_{LDR}, the decrease in cloud albedo (Fig. 5) is between 6 and 10% (marine) and between 11 and 21% (continental). Therefore, in both clouds the dispersion effect on cloud albedo can be seen counting for more than 5%.

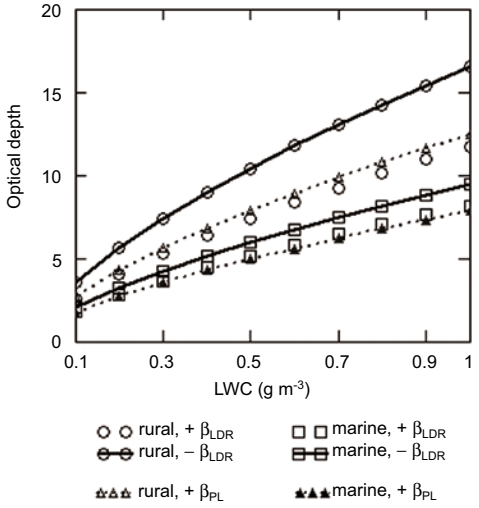

Fig. 3. Dispersion effect on optical depth for a cloud of 100 m thickness, over continental (circles) and marine (squares) areas.

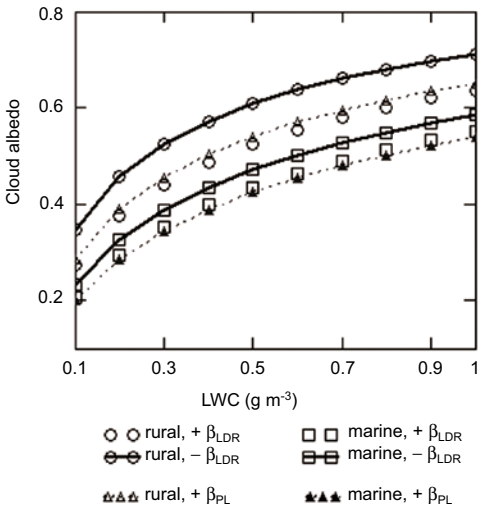

Fig. 4. Dispersion effect on cloud albedo over continental (circles) and marine (squares) areas (thickness of cloud = 100 m).

3.4 Albedo computations with dispersion included in scattering asymmetry factor

In the previous sections, we performed the calculations taking into account the dispersion only in the effective radius, and cloud albedo has been obtained considering a constant value of 0.85 for

the scattering asymmetry factor g. We have repeated calculations but considering that dispersion to be also included in g through Eq. 18. The corresponding relative decrease in cloud albedo for both cloud types is also plotted in Figure 5. It can be seen the important effect that inclusion of dispersion in both r_{eff} and g has on cloud reflectivity: in both types of clouds, the dispersion effect could lead to a relative change in cloud reflectivity for more than 20%. For the same liquid water content, the variability in cloud droplet concentration (from 60 to 319 cm^{-3}) determines variability in albedo of up to 3%.

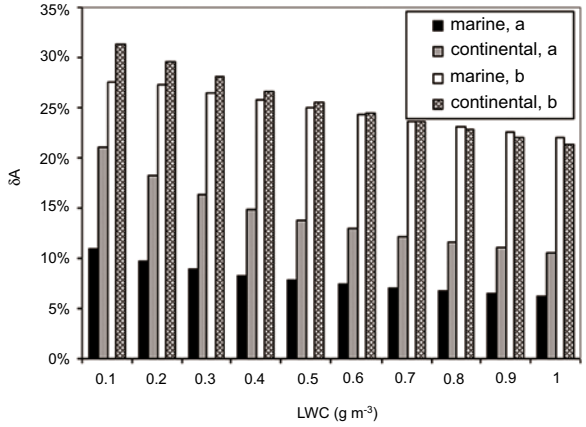

Fig. 5. Cloud albedo percentage difference as a result of dispersion effect (β_{LDR}, eq. 12) for continental and marine clouds. Albedo has been estimated using β_{LDR} in $_{reff}$ (a), and β_{LDR} in both r_{eff} and g (b).

3.5 Comparison with SCAR-B and ASTEX results

The relationship between r_{eff} and LWC for stratocumulus clouds, obtained by Reid *et al.* (1999) from samples analyzed during Smoke, Clouds and Radiation-Brazil (SCAR-B) and Atlantic Stratocumulus Transition Experiment (ASTEX) projects, have been used to compare our results. Their formulas (9 and 19) have been obtained averaging numerous samples, covering a range of droplet concentrations from 100 to 1400 cm^{-3}, and LWC from 0.05 to 2 g m^{-3} in SCAR-B; during ASTEX, droplets concentrations were from less than 100 to 400 cm^{-3}, and LWC varied from 0.01 to 1.6 g m^{-3}. Figure 6 shows the calculated (β_{LDR}-scaled and non-scaled) effective radius compared with the independently measured effective radius by Reid *et al.* (1999).

The calculated cloud albedo, when relative dispersion has been considered, shows better agreement with the estimated cloud albedo from measured effective radius in SCAR-B project than the cloud albedo calculated without dispersion, for clouds over continental areas (Fig. 7a). In cleaner conditions of marine clouds (Fig. 7b), albedo values when relative dispersion has been considered are higher than those inferred using an effective radius-liquid water content relationship proposed by Reid *et al.* (1999) from ASTEX project when LWC exceeds 0.5 g m^{-3}; only β_{PL}-scaled albedo fits satisfactory within the validity range. The low correlation coefficient of 0.36 of the parameterization obtained Reid *et al.* (1999) may also play a role within.

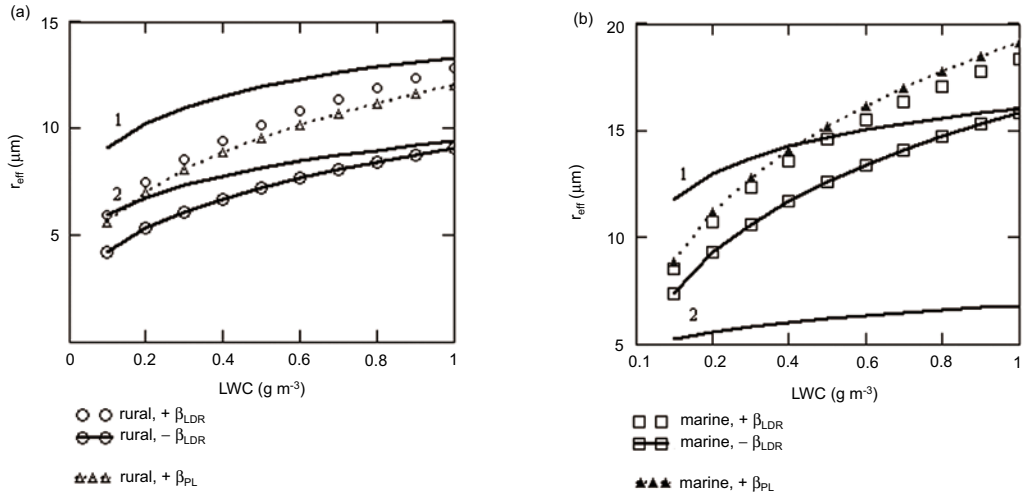

Fig. 6. Cloud droplet effective radius as a function of LWC for (a) clouds over continental areas without dispersion (connected circles) and with dispersion (circles), and the validity range for stratocumulus clouds in SCAR-B (solid lines; line 1, the upper limit of the effective radius; line 2, the lower limit of the effective radius), and for (b) clouds over marine areas and ASTEX project. β_{PL}-effective radius (Peng and Lohmann relationship; eq. 14) for continental clouds (dotted line, triangles) is also presented.

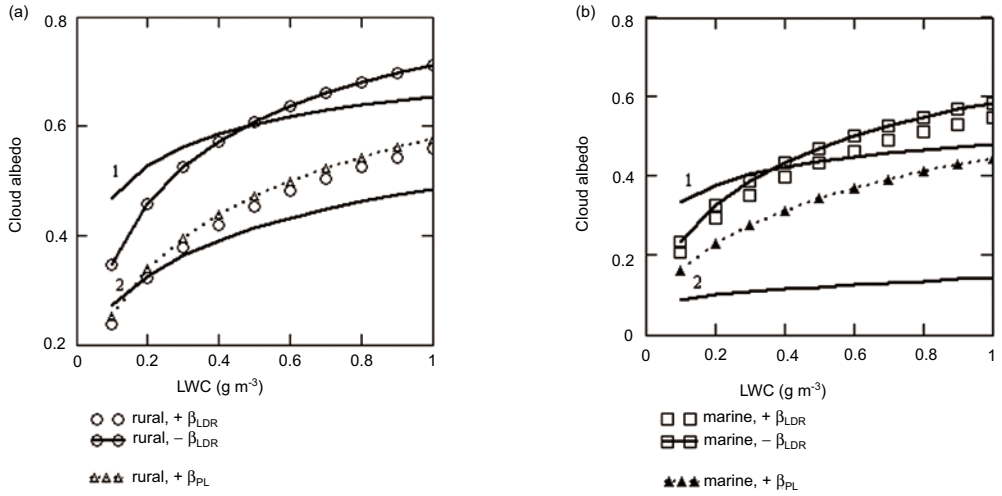

Fig. 7. Cloud albedo as a function of LWC for (a) clouds over continental areas without dispersion (connected circles) and with dispersion (circles), and the validity range for stratocumulus clouds in SCAR-B (solid lines; line 1, the upper limit; line 2, the lower limit), and for (b) clouds over marine areas and ASTEX project. Albedo calculated with β_{PL}-effective radius (Peng and Lohmann relationship; eq. 14) for continental clouds (dotted line, triangles) is also presented.

3.6 Implications for the aerosol first indirect effect

As the first indirect effect is directly related to changes in cloud reflectivity (e.g. Seinfeld and Pandis, 1998), it can be characterized quite well as follows: assuming a constant LWC, a change in droplet number (N) can be roughly related to a change in cloud reflectivity (ΔA):

$$\Delta F_{cloud} = -F_0 \cdot C_c \cdot T_a^2 \cdot \Delta A \tag{20}$$

where F_0 is the incident solar flux (W m^{-2}), C_c is the fractional cloud cover, T_a is the fractional transmittance of the atmosphere, ΔA is the change in cloud albedo. This rough approximation shows that a diminished cloud albedo, due to an enhanced dispersion of cloud droplet spectrum with absolute values (Table III) up to 0.13 (marine) and up to 0.16 (continental), are expected to correspondingly diminish the estimated indirect forcing. Thus, spectral dispersion effects could help to explain the high end of the simulated aerosol first indirect forcing.

Table III. Albedo absolute differences for continental and marine clouds: ΔA_{reff-0} is albedo difference between albedo with dispersion effect included only in effective radius and cloud albedo with no dispersion included; $\Delta A_{(g,reff)-0}$ is albedo difference between albedo with dispersion effect included in both effective radius and in the scattering asymmetry factor and cloud albedo with no dispersion included.

	Marine		Continental	
LWC (g m^{-3})	ΔA_{reff-0}	$\Delta A_{(g,reff)-0}$	ΔA_{reff-0}	$\Delta A_{(g,reff)-0}$
0.1	–0.03	–0.06	–0.07	–0.11
0.2	–0.03	–0.09	–0.08	–0.14
0.3	–0.03	–0.10	–0.09	–0.15
0.4	–0.04	–0.11	–0.09	–0.15
0.5	–0.04	–0.12	–0.08	–0.16
0.6	–0.04	–0.12	–0.08	–0.16
0.7	–0.04	–0.12	–0.08	–0.16
0.8	–0.04	–0.13	–0.08	–0.15
0.9	–0.04	–0.13	–0.08	–0.15
1.0	-0.04	-0.13	-0.08	-0.15

4. Conclusions

This study assesses the variability in cloud albedo that may result from the variability of relative dispersion of cloud droplet spectrum. Using the observed aerosol characteristics, the detailed ARG parameterization to obtain the number of cloud droplets, and a simple cloud model, we found that spectral dispersion may diminish cloud reflectivity by up to 28 (marine) and 31% (continental), with respect to the case when cloud albedo is calculated without considering the dispersion of cloud droplet spectrum.

The calculated cloud albedo scaled by a parameter, which is a function of the relative dispersion of cloud droplet spectrum, shows better agreement with the estimated cloud albedo from measured effective radius in SCAR-B project than the cloud albedo calculated without scaling, for clouds over rural areas. In cleaner conditions of marine clouds, only β_{PL}-scaled albedo fits satisfactory within the validity range of albedo inferred using an effective radius-liquid water content relationship proposed by Reid *et al.* (1999) from ASTEX project. The low correlation coefficient of the parameterization may also play a role within.

Even if our simple estimate of the aerosol effect on cloud reflectivity cannot take all the feedbacks operating in a general or a regional climate model into account, our result shows that spectral dispersion may have important significance for the indirect aerosol effect. We propose that ARG parameterization to be tested in a global or regional climate model when dispersion effect (included in both effective radius and in scattering asymmetry factor) is investigated. The effect produced by the enhancement of ε on cloud reflectivity is evidently large enough to be considered in assessing the indirect aerosol effect, and understanding the relation between ε, N and A will help to reduce the large uncertainty inherent in this effect.

References

Abdul-Razzak H., S. J. Ghan and C. Rivera-Carpio, 1998. A parameterization of aerosol activation, 1. Single aerosol type. *J. Geophys. Res.* **103**, (D6), 6123-6131.

Abdul-Razzak H. and S. J. Ghan, 2000. A parameterization of aerosol activation, 2. Multiple aerosol types. *J. Geophys. Res.* **105**, (D5), 6837-6844.

Abdul-Razzak H. and S. J. Ghan, 2002. A parameterization of aerosol activation, 3. Sectional representation. *J. Geophys. Res.* **107** D3(4026), doi:10.1029/2001JD000483.

Abdul-Razzak H. and S. J. Ghan, 2004. Parameterization of the influence of organic surfactants on aerosol activation. *J. Geophys. Res.* **109** (D03205), doi:10.1029/ 2003JD004043.

Ackerman S., O. B. Toon, D. E. Stevens, A. J. Heymsfield, V. Ramanathan and E. J. Welton, 2000. Reduction of tropical cloudiness. *Science* **288**, 1042-1047.

Albrecht B. A., 1989. Aerosols clouds and microphysics. *Science* **245**, 1227-1230.

Andreae M. O., 1995. Climatic effects of changing atmospheric aerosol levels. In: *World Survey of Climatology.* Vol. 16: *Future Climates of the World* (A. Henderson-Sellers, Ed). Elsevier, Amsterdam, 341-392.

Binkowski F. S. and U. Shankar, 1995. The regional particulate matter model, 1. Model description and preliminary results. *J. Geophys. Res.* **100**,191-26,209.

Bond T. C., D. G. Streets, K. F. Yarber, S. M. Nelson, J.-H. Woo and Z. Klimont, 2004. A technology based inventory of black and organic carbon emissions from combustion. *J. Geophys. Res.,* **109**(D14), 203, doi:10.1029/2003JD003697.

Boucher O. and U. Lohmann, 1995. The sulfate-CCN-cloud albedo effect: a sensitivity study with two general circulation models. *Tellus* **47B**, 281-300.

Bott A., 2000. A numerical model of the cloud-topped planetary boundary layer: influence of the physico-chemical properties of aerosol particles on the effective radius of stratiform clouds. *Atmos. Res*. **53**, 15-27.

Chameides W. L., C. Luo, R. Saylor, D. Streets, Y. Huang, M. Bergin and F. Giorgi, 2002. Correlation between model-calculated anthropogenic aerosols and satellite-derived cloud optical depths: Indication of indirect effect? *J. Geophys. Res.* **107**(D10), doi:10.1029/ 2000JD000208.

Charlson R. J., S. E. Schwartz, J. M. Hales, R. D. Cess, J. A. Jr. Coakley, J. E. Hansen and D. J. Hofmann, 1992. Climate forcing by anthropogenic aerosols. *Science* **255**, 423-430.

Chen Y. and J. E. Penner, 2005. Uncertainty analysis for estimates of the first indirect aerosol effect. *Atmos. Chem. Phys.* **5**, 2935-2948.

Environmental Protection Agency (EPA), 1999. User manual for the EPA third generation air quality modeling system (Models-3 Version 3.0), Rep. EPA-600/R-99/055, Off. of Res. and Dev., U.S. Environ. Prot. Agency, Washington D. C.

Feingold G. and P. Y. Chuang, 2002. Analysis of the influence of film-forming compounds on droplet growth: Implications for cloud microphysical processes and climate. *J. Atmos. Sci.* **59**, 2006-2018.

Flossman A. I., W. D. Hall and H. R. Pruppacher, 1985. A theoretical study of the wet removal of atmospheric pollutants, Part I: The redistribution of aerosol particles captured through nucleation and impaction scavenging by growing cloud drops. *J. Atmos. Sci.* **42**, 583-606.

Fountoukis C. and A. Nenes, 2005. Continued development of a cloud droplet formation parameterization for global climate models. *J. Geophys. Res.* **110**, D11212, doi:10.1029/ 2003JD004324.

Ghan S. J., C. C. Chuang and J. E. Penner, 1993. A parameterization of cloud droplet nucleation, Part I, Single aerosol type. *Atmos. Res.* **30**, 197-221.

Ghan S. J., L. R. Leung and Q. Hu, 1997. Application of cloud microphysics to NCAR community climate model. *J. Geophys. Res.* **102**, 16,507-16,527.

Ghan S. J., R. C. Easter, E. G. Chapman, H. Abdul-Razzak, Y. Zhang, L. R. Leung, N. Laulainen, R. D. Saylor and R. Zaveri, 2001a. A physically-based estimate of radiative forcing by anthropogenic sulfate aerosol. *J. Geophys. Res.* **106**, 5279-5293.

Ghan S. J., N. S. Laulainen, R. C. Easter, R. Wagener, S. Nemesure, E. G. Chapman, Y. Zhang and L. R. Leung, 2001b. Evaluation of aerosol direct radiative forcing in MIRAGE. *J. Geophys. Res.* **106**, 5295-5316.

Ghan S. J., R. C. Easter and F.-M. Breon, 2001c. Evaluation of aerosol indirect radiative forcing in MIRAGE. *J. Geophys. Res.* **106**, 5317-5334.

Giorgi F., 1986. Development of an atmospheric model for studies of global budgets and effects of airborne particulate material, Ph.D. thesis. Georgia Institute of Technology, Atlanta, GA, USA, 226 pp.

Godish T., 1997. *Air Quality* (3rd Ed.). CRC Press LLC, Boca Raton, Florida, USA, 448 pp.

Gultepe I. and G. A. Isaac, 1999. Scale effects on averaging of cloud droplet and aerosol number concentrations: observations and models. *J. Climate* **12**, 1268-1279.

Han Q., W. B. Rossow and A. A. Lacis, 1994. Near-global survey of effective droplet radii in liquid water clouds using ISCCP data. *J. Climate* **7**, 465-497.

Hansen J. E. and L. D. Travis, 1974. Light scattering in planetary atmospheres. *Space Sci. Rev.* **16**, 527-610.

Hansen J. E., M. Sato and R. Ruedy, 1997. Radiative forcing and climate response. *J. Geophys. Res.* **102**, 6831-6864.

Haywood J. and O. Boucher, 2000. Estimates of the direct and indirect radiative forcing due to tropospheric aerosols: A review. *Rev. Geophys.* **38**, 513-543.

Haywood J. M., and K. P. Shine, 1995. The effect of anthropogenic sulfate and soot aerosol on the clear-sky planetary radiation budget. *Geophys. Res. Lett.* **22**, 603-606.

Heymsfield A. J. and R. M. Sabin, 1989. Cirrus crystal nucleation by homogeneous freezing of solution droplets. *J. Atmos. Sci.* **25**, 2252-2264.

Hoppel W. A and G. M. Frick, 1990. Submicron aerosol size distributions measured over the tropical and South Pacific. *Atmos. Environ.* **24A**, 645-659.

Hudson J.G. and S. S. Yum, 1997. Droplet spectral broadening in marine stratus. *J. Atmos. Sci.* **54,** 2642-2654.

IPCC, 2001. Houghton, J. T.,Y. Ding, D. J. Griggs, M. Noguer, P. J. van der Linden, X. Dai, K. Maskell, and C. A. Johnson (Eds.), Climate Change 2001: The Scientific Basis. Contribution of Working Group I to the 3rd Assessment Report of the Intergovernmental Panel on Climate Change. Cambridge University Press, Cambridge, UK, 881 pp.

Jaenicke R., 1988. Aerosol physics and chemistry. In: *Zahlenwerte und Funktionen aus Naturwissenschaften und Technik* (Landolt-Boernstein, Ed.), Serie V, Vol. 4b, Springer, 391-457.

Jonas P. R., R. J. Charlson and H. Rodhe, 1995. Aerosols. In: *Climate Change 1994: Radiative Forcing of Climate and an Evaluation of the IS92 Emission Scenarios* (J. T. Houghton, L. G. Meira Filho, J. Bruce, L. Hoesong, B. A. Callander, E. F. Haites, N. Harris and K. Maskel, Eds). Cambridge University Press, Cambridge, UK, 127-162.

Kanakidou M., J. H. Seinfeld, S. N. Pandis, I. Barnes, F. J. Dentener, M. C. Facchini, R. van Dingenen, B. Ervens, A. Nenes, C. J. Nielsen, E. Swietlicki, J. P. Putaud, Y. Balkanski, S. Fuzzi, J. Horth, G. K. Moortgat, R. Winterhalter, C. E. L. Myhre, K. Tsigaridis, E. Vignati, E. G. Stephanou and J.Wilson, 2005. Organic aerosol and global climate modelling: a review. *Atmos. Chem. Phys.* **5**, 1053-1123.

Kiehl J. T. and H. Rodhe, 1995. Modeling geographical and seasonal forcing due to aerosols. In: *Aerosol Forcing of Climate* (R. J. Charlson and J. Heintzenberg, Eds.), J. Wiley and Sons, NY, USA, 281-296.

Lacis A. A. and J. E. Hansen, 1974. A parameterization for the absorption of solar radiation in the Earth's atmosphere. *J. Atmos. Sci.* **31**, 118-133.

Lance S., A. Nenes and T. Rissman, 2004. Chemical and dynamical effects on cloud droplet number: Implications for estimates of the aerosol indirect effect. *J. Geoph. Res.* **109**, D22208, doi:10.1029/2004JD004596.

Lee I. Y., G. Haenel and H. R. Pruppacher, 1980. A numerical determination of the evolution of cloud drop spectra due to condensation on natural aerosol particles. *J. Atmos. Sci.* **37**, 1840-1853.

Liu Y. and P. H. Daum, 2002. Indirect warming effect from dispersion forcing. *Nature* **419**, 580-581.

Liu Y., P. H. Daum and S. S. Yum, 2006. Analytical expression for the relative dispersion of the cloud droplet size distribution. *Geophys. Res. Lett.* **33**, L02810, doi:10.1029/ 2005GL024052.

Lohmann U., J. Feichter, C. C. Chuang and J. E. Penner, 1999. Prediction of the number of cloud droplets in the ECHAM GCM. *J. Geophys. Res.* **104**, 9169-9198.

Lohmann U., J. Feichter, J. E. Penner and R. Leaitch, 2000. Indirect effect of sulfate and carbonaceous aerosols: a mechanistic treatment. *J. Geophys. Res.* **105**, 12193-12206.

Lohmann U. and J. Feichter, 2005. Global indirect aerosol effects: A review. *Atmos. Chem. Phys.* **5**, 715-737.

Lowenthal D. H, R. D. Borys, T. W. Choularton, K. N. Bower, M. J. Flynn and M. W. Gallagher, 2004. Parameterization of the cloud droplet-sulfate relationship. *Atmos. Environ.* **38**, 287-292.

Lu M.-L. and J. H. Seinfeld, 2006. Effect of aerosol concentration on cloud droplet dispersion: A large-eddy simulation study and implications for aerosol indirect forcing. *J. Geophys. Res.* **111** (D02207), doi: 10.1029/2005/JD006419.

Martin G. M., D. W. Johnson and A. Spice, 1994. The measurement and parameterization of effective radius of droplets in warm stratocumulus clouds. *J. Atmos. Sci*. **51**, 1823-1842.

McFiggans G., P. Artaxo, U. Baltensperger, H. Coe, M. C. Facchini, G. Feingold, S. Fuzzi, M. Gysel1, A. Laaksonen, U. Lohmann, T. F. Mentel, D. M. Murphy, C. D. O'Dowd, J. R. Snider and E. Weingartner, 2006. The effect of physical and chemical aerosol properties on warm cloud droplet activation. *Atmos. Chem. Phys.* **6**, 2593-2649.

Menon S., V. K. Saxena, P. Durkee, B. N. Wenny and K. Nielsen, 2002. Role of sulfate aerosols in modifying the cloud albedo: a closure experiment. *Atmos. Res.* **61**, 169-187.

Miles N. L., J. Verlinde and E. E. Clotiaux, 2000. Cloud droplet size distributions in low-level stratiform clouds. *J. Atmos. Sci.* **57**, 295-311.

Nenes A., S. Ghan, H. Abdul-Razzak, P. Y. Chuang and J. H. Seinfeld, 2001. Kinetic limitations on cloud droplet formation and impact on cloud albedo. *Tellus B* **53**, 133-149.

Nenes A. and J. H. Seinfeld, 2003. Parameterization of cloud droplet formation in global models. *J. Geophys. Res.* **108**(D14), 4415, doi: 10.1029/2002JD002911.

Paluch I. R. and D. H. Lenschow, 1992. Comment on "Measurements of Aitken nuclei and cloud condensation nuclei in the marine atmosphere and their relation to the DMS-cloud-climate hypothesis" by Hegg, D. A., L. F. Radke, and P. V. Hobbs. *J. Geophys. Res.* **97**, 7657-7658.

Peng Y., U. Lohmann, R. Leaitch, C. Banic and M. Couture, 2002. The cloud albedo-cloud droplet effective radius relationship for clean and polluted clouds from RACE and FIRE.ACE. *J. Geophys. Res.* **107**, doi:10.1029/2000JD000281.

Peng Y. and U. Lohmann, 2003. Sensitivity study of the spectral dispersion of the cloud droplet size distribution on the indirect aerosol effect. *Geophys. Res. Lett.* **30** (10), 1507, doi:10.1029/2003GL017192.

Pincus R. and M. A. Baker, 1994. Effect of precipitation on the albedo susceptibility of clouds in the marine boundary layer. *Nature* **372**, 250-252.

Pruppacher H. R. and J. D. Klett, 1997. *Microphysics of clouds and precipitation*. Kluwer Academic Publishers, Netherlands, 954 pp.

Putaud J.-P., F. Raes, R. van Dingenen, E. Brueggemann, M.-C. Facchini, S. Decesari, S. Fuzzi, R. Gehrig, C. Hueglin, P. Laj, G. Lorbeer, W. Maenhaut, N. Mihalopoulos, K. Mueller, X. Querol, S. Rodríguez, J. Schneider, G. Spindler, H. ten Brink, K. Trseth and A. Wiedensohler, 2004. A European aerosol phenomenology—2: chemical characteristics of particulate matter at kerbside, urban, rural and background sites in Europe. *Atmos. Environ.* **38**, 2579-2595.

Qian Y, L. R. Leung, S. J. Ghan and F. Giorgi, 2003. Regional climate effects of aerosols over China: modeling and observation. *Tellus B* **55**, 914-934.

Ramanathan V., P. J. Crutzen, J. Lelieveld, A. P. Mitra, D. Althausen, J. Anderson, M. O. Andreae, W. Cantrell, G. R. Cass, C. E. Chung, A. D. Clarke, J. A. Coakley, W. D. Collins, W. C. Conant, F. Dulac, J. Heintzenberg, A. J. Heymsfield, B. Holben, S. Howell, J. Hudson, A. Jayaraman, J.T. Kiehl, T. N. Krishnamurti, D. Lubin, G. McFarquhar, T. Novakov, J. A. Ogren, I. A. Podgorny, K. Prather, K. Priestley, J. M. Prospero, P. K. Quinn, K. Rajeev, P. Rasch, S. Rupert, R. Sadourny, S. K. Satheesh, G. E. Shaw, P. Sheridan and F. P. J. Valero, 2001. Indian Ocean Experiment: An integrated analysis of the climate forcing and effects of the great Indo-Asian haze. *J. Geophys. Res.* **106** (D22), 28371-28398.

Reid J. S., P. V. Hobbs, A. L. Rangno and D. A. Hegg, 1999. Relationships between cloud droplet effective radius, liquid water content, and droplet concentration for warm clouds in Brazil embedded in biomass smoke. *J. Geophys. Res.* **104**, 6145-6153.

Rissman T., A. Nenes and J. H. Seinfeld, 2004. Chemical amplification (or dampening) of the Twomey effect: Conditions derived from droplet activation theory. *J. Atmos. Sci*. 61, 919-930.

Roelofs G., J. Lelieveld and L. Ganzeveld, 1998. Simulation of global sulfate distribution and the influence on effective cloud drop radii with a coupled photochemistry-sulfur cycle model. *Tellus B* **50**, 224-242.

Rotstayn L. D. and Y. Liu, 2003. Sensitivity of the first indirect aerosol effect to an increase of cloud droplet spectral dispersion with droplet number concentration. *J. Climate* **16**, 3476-3481.

Seinfeld J. H. and S. N. Pandis, 1998. *Atmospheric chemistry and physics. From air pollution to climate change.* Willey-Interscience, New York, 1326 pp.

Slingo A., 1989. A GCM parameterization for the shortwave radiative properties of clouds. *J. Atmos. Sci.* **46**, 1419-1427.

Srivastava R. C., 1991. Growth of cloud drops by condensation: Effect of surface tension on the dispersion of drop sizes. *J. Atmos. Sci.* **48,** 1596-1605.

Stephens G. L., 1978. Radiation profiles in extended water clouds. II: Parametrization schemes. *J. Atmos. Sci.* **35**, 2123-2132.

Taylor K. E. and J. E. Penner, 1994. Response of the climate system to atmospheric aerosols and greenhouse gases. *Nature* **369**, 734-737.

Twomey S., 1959. The nuclei of natural cloud formation, Part II: The supersaturation in natural clouds and the variation of cloud droplet concentration. *Geofis. Pura Appl.* **43**, 243-249.

Twomey S., 1974. Pollution and the planetary albedo. *Atmos. Environ.* **8**, 1251-1256.

Yu H., Y. J. Kaufman, M. Chin, G. Feingold, L. A. Remer, T. L. Anderson, Y. Balkanski, N. Bellouin, O. Boucher, S. Christopher, P. DeCola, R. Kahn, D. Koch, N. Loeb, M.S. Reddy, M. Schulz, T. Takemura and M. Zhou, 2006. A review of measurement-based assessments of the aerosol direct radiative effect and forcing. *Atmos. Chem. Phys.* **6**, 613-666.

Wood R., S. Irons and P. R. Jonas, 2002. How important is the spectral ripening effect in stratiform boundary layer clouds? Studies using simple trajectory analysis. *J. Atmos. Sci.,* **59,** 2681-2693.

Zhang Y., R. C. Easter, S. J. Ghan and H. Abdul-Razzak, 2002. Impact of aerosol size representation on modeling aerosol-cloud interactions. *J. Geophys. Res.* **107**(D21), 4558, doi:10.1029/2001JD001549.